The Journal of Experimental Biology 212, 1021-1031
Published by The Company of Biologists 2009
doi:10.1242/jeb.023507

Movement encoding by a stretch receptor in the soft-bodied caterpillar, *Manduca sexta*

Michael A. Simon* and Barry A. Trimmer
Department of Biology, Tufts University, Medford, MA 02155, USA
*Author for correspondence (e-mail: Michael.Simon@tufts.edu)

Accepted 6 January 2009

SUMMARY

In a wide variety of animals, stretch receptors provide proprioceptive feedback for motion control. However, for animals that lack a stiff skeleton, it is unclear what information is being detected and how this is incorporated into behavior. Because such animals can change their body shape from moment-to-moment, information about body configuration could be particularly important for coordination. This study uses larval stage Lepidoptera (*Manduca sexta*) to examine how the longitudinal stretch receptor organ (SRO) responds to behaviorally appropriate movements. We characterized the responses of the SRO to changes in strain using magnitudes and velocities matching those seen physiologically. We found that the SRO response characteristics are compatible with the regulation of stance and with the defensive response to noxious stimuli. However, we also found that movements during crawling produce SRO responses that are dominated by the interdependence of phasic, tonic and slowly adaptive components. Ablation of stretch receptors in the proleg-bearing, fourth abdominal segment did not have any observable effect on behaviors, which suggests that the SROs are not essential for coordinating overt movements. We discuss the implications of these findings in the context of specific behaviors, and explore how the SRO response might be utilized during animal behavior.

Supplementary material available online at http://jeb.biologists.org/cgi/content/full/212/7/1021/DC1

Key words: locomotion, *Manduca sexta*, mechanosensors.

INTRODUCTION

Stretch receptors guide muscle control and provide proprioceptive feedback in organisms throughout the animal kingdom. Vertebrates and arthropods with stiff skeletons can use activity in stretch receptors and force sensors (e.g. Golgi tendon organs) to determine limb position, joint movements and applied forces throughout a motor task. In vertebrates, stretch-sensitive mechanosensors entrain rhythmic swimming patterns [e.g. in lamprey (Tytell and Cohen, 2008)], signal inspiration and lung volume [e.g. in birds (Bouverot, 1978); in mammals (Paintal, 1973)], coordinate the timing and magnitude of muscle force generation during walking (Stein et al., 2000) and compensate for perturbations in gait due to ground irregularities and other external factors (Dietz et al., 2002). Stretch receptors also take a variety of forms in invertebrates. The muscle receptor organ (MRO) of *Cherax destructor*, for example, consists of pairs of stretch receptors that coordinate slow abdominal movement and maintain tail position (Fields and Kennedy, 1965) and engage abdominal extension following the tail-flip response (Cattaert and Le Ray, 2001). Abdominal stretch receptors in the mosquito (Gwadz, 1969) and *Rhodnius prolixus* (Anwyl, 1972) regulate feeding behavior to prevent abdominal rupture during blood meals. And, motoneurons coordinating dorsal–ventral sinusoidal movement in the nematode, *Caenorhabditis elegans*, appear to be stretch sensitive, suggesting a role in coordinating forward and backward locomotion (O'Hagan et al., 2005; Syntichaki and Tavernarakis, 2004).

Invertebrate stretch receptors can be anatomically classified as either muscle-associated or non-muscle-associated. One functional distinction between the two types is that the response of muscle-associated stretch receptors can be modulated in the periphery by efferent feedback. In the crustacean MRO, pairs of innervated receptor muscles provide feedback on extensor muscle movement, with separate 'fast' and 'slow' fibers responding quickly or slowly to motoneuron activation and adapting quickly or slowly to changes in stretch position, respectively (Alexandrowicz, 1967; Kuffler, 1954). Slow fibers respond tonically to degrees of stretch whereas fast fibers respond phasically and briefly to rapid stretch. In both cases, the associated muscle fibers are innervated by the same motoneurons that innervate nearby non-sensory muscle fibers (Fields, 1966; Fields and Kennedy, 1965). The presence of separate tonic and phasic sensors is not universal among invertebrate stretch receptors, however. For example, the coxo-trochantal MRO (CTMRO) of the locust is a muscle-associated receptor that is innervated by only a single sensory neuron (Braunig and Hustert, 1983). The associated muscle of the CTMRO is stimulated by nearby non-muscle-associated proprioceptors and adjacent joints to maintain sensory range (Braunig and Hustert, 1985). Such efferent feedback acts peripherally at the site of the sensor in muscle-associated stretch receptors. By contrast, the non-muscle-associated leg chordotonal organ in locust senses stretch in an associated connective tissue that cannot be regulated by peripheral efferent feedback.

Because such non-muscle-associated stretch receptors sense a connection between hinged rigid points, the range of motion for these sensors is fixed. In soft-bodied animals, although some rigid points exist [e.g. sclerotinized cuticle (Snodgrass, 1935) and quasi-jointed structures (Sumbre et al., 2005)], such points are rare and movements generally have more degrees of freedom. We expect that soft-bodied animals would require stretch sensors with a greater dynamic range than that available through non-muscle-associated stretch sensors. Such soft-bodied animals include the caterpillar of the tobacco hawkmoth, *Manduca sexta*, and other well-documented Lepidoptera

such as *Antheraea pernyii* (Osborne and Finlayson, 1965; Weevers, 1965) and *Hyalophora cecropia* (Beckel, 1958; Libby, 1961). The stretch receptor organ (SRO) of *Antheria pernyii* responds tonically to slow stretch and phasically to rapid stretch. Unlike the crustacean MRO, the stretch receptors described in *Antherea* (Osborne and Finlayson, 1965) and in the locust (Braunig and Hustert, 1983) respond both tonically and phasically through the same sensory neuron and are innervated by only one efferent motoneuron. This simplicity of structure and control prompts questions about how the central nervous system (CNS) integrates tonic and phasic information in the coordination of behavior.

In Lepidoptera, the most likely candidates for stretch feedback during locomotion are the large longitudinal stretch receptors that span the length of each abdominal segment and run parallel to the major intersegmental muscles [illustrated in *Hyalophora cecropia* (Beckel, 1958)] (Fig. 1B). This SRO appears to signal the length of tissues spanning its insertion points. Past studies have shown that the SRO firing rate reflects both segment length and the velocity of stretch (Lowenstein and Finlayson, 1960; Weevers, 1965). When the SRO is held in a fixed position or is stretched slowly, the stretch receptor sensory neuron (SRSN) fires tonically, at a rate proportional to the length of the SRO. When the SRO is stretched rapidly (approximately $>0.5\,l\,s^{-1}$), the SRSN fires phasically and at a rate proportional to the stretch velocity and far greater than expected for a given position. The location and function of this SRO suggest that it serves a proprioceptive function during abdominal movement. SRO stimulation results in stretch reflexes [in *Manduca* (Tamarkin and Levine, 1996); in *Antherea* (Weevers, 1966c)] but it is unclear how such reflexes are incorporated into spontaneous movements.

Recognizing that realistic animal movements are more complicated than changes in length between fixed points, we used several experimental approaches to characterize the SRO and its role in behavior in the soft-bodied animal. First, we characterized the tonic and phasic responses of the longitudinal SRO of *Manduca sexta* using time- and position-varying stimuli. To compare *Manduca* SRO with other stretch receptors, we began by examining the functional response of the SRO to stereotyped stimuli such as stretch-and-hold stimuli. Second, we repeated steady-state stretch experiments, paying particular attention to transients in the functional response that could modify the overall response of the SRO during behavior. Third, we expected that stretch amplitude, and not just position and speed, may affect rapid SRO responses. Therefore, we tested the effect of degree of stretch on SRO phasic response, looking for evidence of response thresholds. Additionally, past studies have shown that non-linear analysis is an effective way to examine the full response of a mechanosensor to a wide spectrum of stimuli [in crabs (DiCaprio, 2003; French, 1980); in cockroaches (French and Wong, 1977; Gamble and DiCaprio, 2003); in locust (Kondoh et al., 1995); in cats (Kroller, 1993); in flies (Marmarelis and Mccann, 1973); in chinchilla (Recio-Spinoso et al., 2005)]. We used Wiener kernel analysis to test our results against those observed in other organisms. Furthermore, to examine the role of the SRO in behavior, we watched *Manduca* performing spontaneous and evoked behavior following real or sham surgical SRO ablations. Finally, in the present study, we discuss the implications of these findings in the context of specific behaviors, including postural maintenance (stance), crawling and the strike response to noxious stimuli.

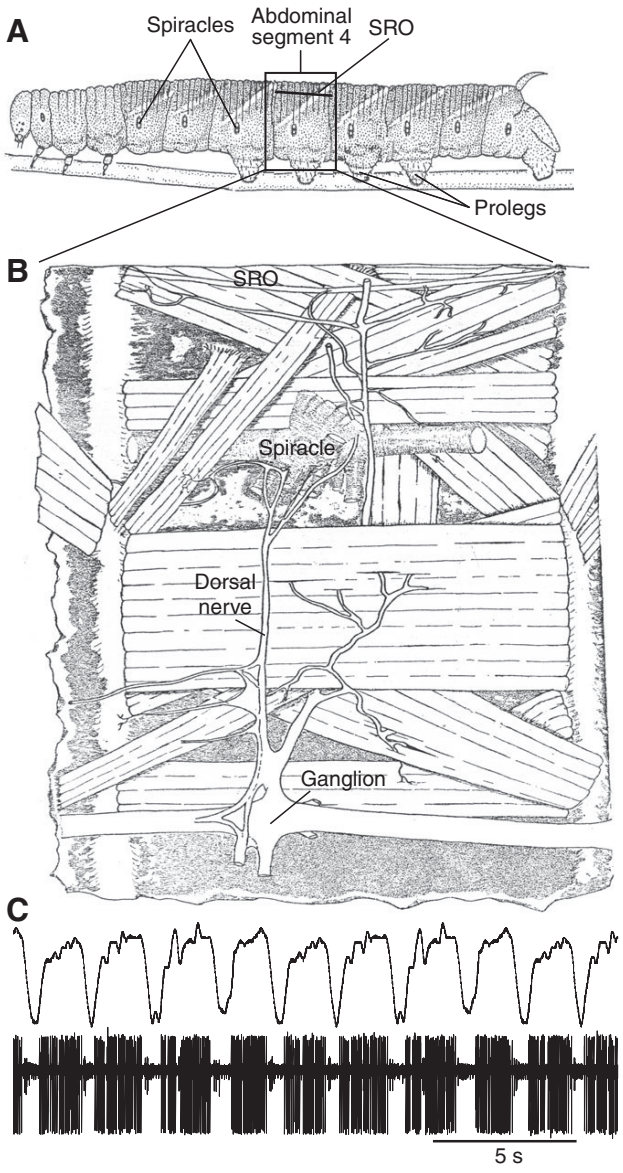

Fig. 1. *Manduca sexta* larvae used in these experiments. (A) Lateral view of *M.* sexta. The animal is composed of a head, three thoracic segments, seven abdominal segments and a terminal segment. The experiments described in the present study examine the stretch receptor organ (SRO) in the abdominal segments. (B) The dorsal lateral nerve (DNL) innervates dorsal musculature, as well as the longitudinal SRO, which attaches to the body wall and spans the entire segment. Adapted from a drawing of *Hyalophora cecropia* (Beckel, 1958), whose major anatomical features are identical to those of *Manduca*. (C) Recordings of SRO activity during repeated strain cycling derived from the kinematics of crawling. The upper trace shows the length of cuticle-bearing SRO, the lower trace shows DNL activity measured *via* an extracellular electrode. Representative sample.

MATERIALS AND METHODS

Raising animals

Larvae of the tobacco hornworm *Manduca sexta* (Lepidoptera: Sphingidae, L.) (Fig. 1), from a colony at Tufts University, Medford, MA, USA, were raised in a 17 h:7 h light:dark cycle at 27°C on an artificial diet (Bell and Joachim, 1976). Male and female fifth-instar larvae, in the first or second day following their molt, were used for the experiments described in the present study.

Kinematics

In all cases, animals were anesthetized by chilling in ice for 30 min or longer. When observing crawling kinematics, muscle insertion points on proleg-bearing abdominal segments were marked with

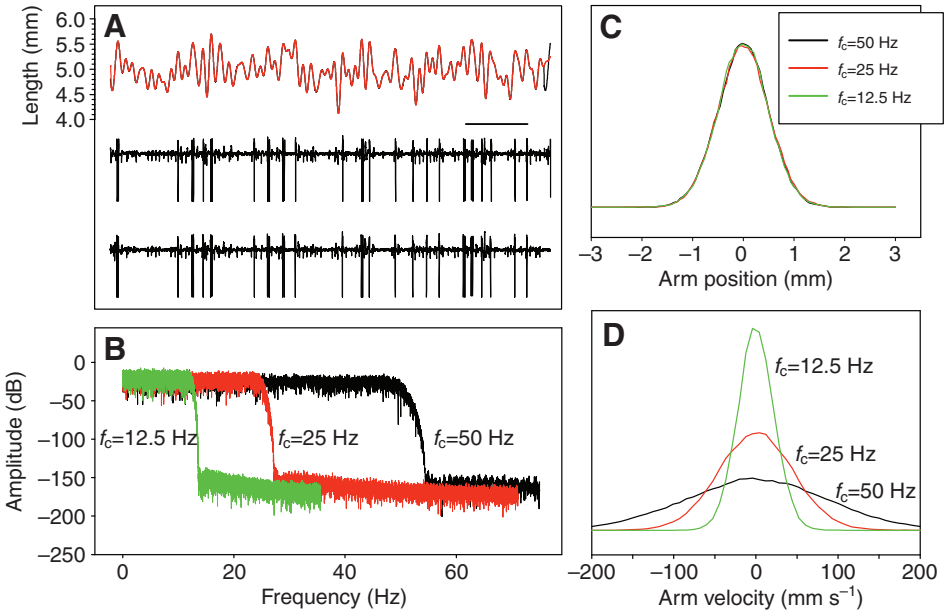

Fig. 2. Validation of Gaussian white noise (GWN) stimulus. (A) Stimulus was generated with desired cutoff frequency (f_c) and then upsampled and filtered to prevent stretch receptor organ (SRO) damage. The upper trace is a sample stimulus as measured by the ergometer on two repeated outputs, labeled red and black. The lower traces are responses to the sample stimulus on two occasions. Note the repeatability of the response to stimulus. Scale bar=200 ms. (B) Frequency spectrum of stimuli at specific f_c. (C) Histogram of arm position values in GWN. All three f_c generate nearly identical position distributions. (D) Histogram of stretch velocity at f_c.

small (<200 µm) fluorescent latex beads (e.g. see Movie 1 in supplementary material). Two digital video cameras (Canon, Ota, Tokyo, Japan) then recorded crawling movements. When observing strike reflex kinematics, intersegmental boundaries were marked using fluorescent paint. One digital camera, directly over and pointing down on the animal, recorded horizontal side-to-side flexing during strike (see Movies 2A,B in supplementary material). Animals were gently squeezed on their dorsal horn or their terminal ganglion with large forceps to instigate the strike reflex. Digital video recordings of movements were converted into 3-D (crawling) or 2-D (strike reflex) kinematic mappings by linear transformation software (APAS, Ariel Dynamics, Trabuco Canyon, CA, USA).

Electrophysiology

Except where noted, animals were dissected in a standard preparation. Larvae were anesthetized by chilling in ice for 30 min or longer. Chilled animals were dissected along the midline from the dorsal horn to the thoracic ganglia and the head capsule. Animals were pinned cuticle-side down in an elastomer-lined dish, covered with modified Miyazaki insect saline (Trimmer and Weeks, 1991) and the terminal and parathoracic ganglia were removed. Trachea and fat bodies were then removed to clearly expose the underlying musculature.

The SRO is connected to the CNS *via* the dorsal lateral nerve (DNL) (Fig. 1B). The ventral muscles were cut in order to expose the DNL, and the posterior and anterior DNL branches were cut close to the dorsal nerve. The ganglion for the segment under study, typically A4, was disconnected from the remainder of the nerve cord and body wall, leaving it still connected to the stretch receptor and dorsal musculature *via* the DNL. The entire dorsal hemisegment, composed of the appropriate segment and the two adjacent segments on either side, was entirely removed from the animal, with the DNL and ganglion still attached, and transferred to a separate elastomer-lined dish containing saline.

One side of the preparation was pinned cuticle-side up in the dish at one of the adjacent segments. Cuticle on the opposite end of the stretch receptor was pierced with a pin connected to the arm of a computer-controlled ergometer (Cambridge Technology, Watertown, MA, USA) and the tissue was stretched to approximately the resting length of the segment in the intact animal following chilling. The displacement of the hook and the force exerted by the ergometer were controlled by a customized LabVIEW program (National Instruments Corp., Austin, TX, USA), which was capable of generating arbitrary length and force signals.

DNL activity was monitored by an extracellular suction electrode placed on the nerve and close to the SRO and amplified by a differential amplifier (A-M Systems, Sequim, WA, USA). The DNL was cut proximal to the electrode so that only afferent activity would be recorded. Afferent activity was sampled at ≥10 kHz and recorded by a computer-based data acquisition system (Dataq DI-720 and Windaq Software, Dataq Instruments, Akron, OH, USA). Spikes were identified by template or threshold detection using DataView software (W. J. Heitler, University of St Andrews, UK). Except where otherwise noted, instantaneous spike frequencies were determined from inter-spike intervals. Phasic activity was typically quantified by mean maximum phasic frequency, which was the mean of the maximum frequency observed during positive stretching within at least 10 consecutive stretches.

Wiener kernel analysis

Preparations were mechanically stimulated with Gaussian white noise (GWN) generated by a GWN function in LabVIEW (National Instruments Corp.) with three different cutoff frequencies (f_c) during the span of one trial. By using multiple f_c, we hoped to capture any differences between response characteristics, particularly non-stationary or adaptive responses to the higher frequency signals (Kondoh et al., 1995; Kroller, 1993). The GWN signal was upsampled to the ergometer-length input rate (10 kHz) and passed through a low-pass (10 kHz) finite impulse response (FIR) filter to avoid damage to the preparation. Preparations were stimulated for approximately 90 s at each f_c, twice the duration necessary for 95% complete tonic adaptation at median adaptation time constant (see Discussion). Between GWN stimuli, the preparations were held at rest length for approximately 90 s.

Preparation lengths, as measured by an ergometer, and evoked spike response were sampled as discussed earlier (Fig. 2A) and then downsampled to 2 kHz. SRO-evoked spikes were converted to delta functions one sample long (Marmarelis, 1978). First- and second-

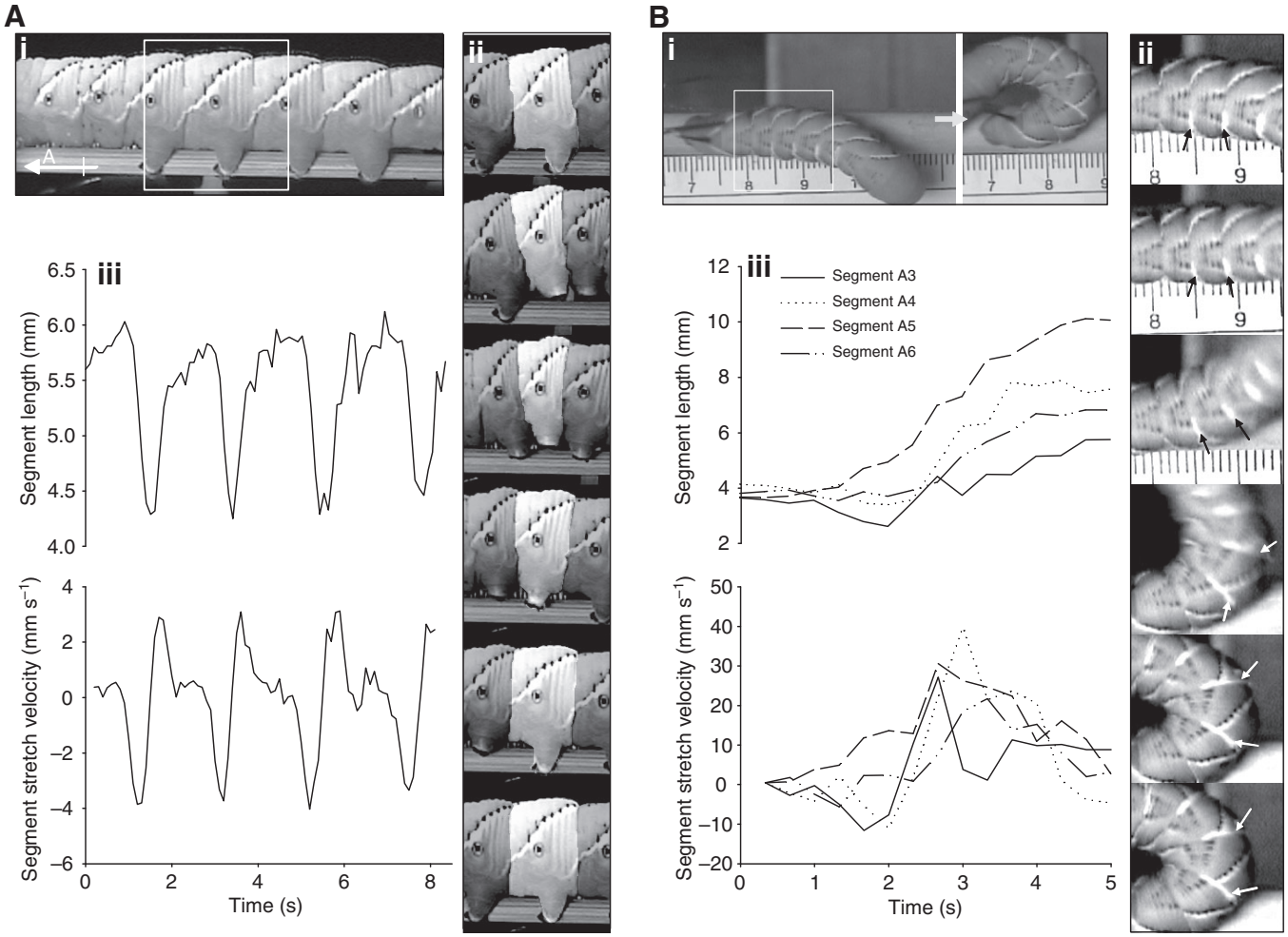

Fig. 3. Kinematics of crawling and strike behaviors. (A) Crawling by *M. sexta* on a dowel. (i) Four abdominal segments shown in lateral view, anterior to the left, dorsal-side up. White box shows the area visualized in (ii). Arrow A indicates anterior. (ii) Images of fourth abdominal segment during a single crawl, at 0.33 s intervals. The fourth segment is highlighted to illustrate segment compression and expansion during a crawl cycle. (iii) Segment length was calculated from the length of dorsal interior muscle during crawling (see Movie 1 in supplementary material for crawling animal with fluorescent markers). Segment stretch velocity was computed as time-averaged time-derivative of segment length. Representative sample. (B) Strike response to pinching on terminal segment. (i) Upon pinching, the animal swings its head either left or right to strike at the stimulus source. Segment boundaries were painted for identification. Example shown is of a strike away from the measured side. White box shows the area visualized in (ii). (ii) Images of fifth abdominal segment during a strike away from the measured side, in 100 ms intervals. Arrows indicate segment boundaries. (iii) Segment length was calculated as the linear distance between approximate stretch receptor organ (SRO) attachment points. Segment velocity was calculated as the time-averaged time-derivative of segment length. Length and velocity may exceed those shown due to an unknown level of muscle curvature during strike. Note the different time and velocity scales for the two different behaviors. Representative samples.

order Wiener kernels were generated from 20 s-long stimulus/response data series, beginning 30 s after the start of a stimulus, using traditional cross-correlation techniques (French and Marmarelis, 1999; Gamble and DiCaprio, 2003; Marmarelis, 1978) and were computed by Lysis 7.1 software (BMSR-USC, Los Angeles, CA, USA). Results were based on recordings from individual SROs from 12 different animals stimulated by GWN with f_c=12.5, 25 and 50 Hz, in that order (Fig. 2B–D). These values were chosen as they encompassed the range of velocities expected in behaviors of interest (Fig. 3).

Surgical SRO ablations

To confirm mobility and health, fifth-instar *Manduca sexta* in the first day post-molt were observed for several hours crawling on various substrates in different orientations. These animals were then chilled on ice for at least 20 min. Holes were poked in the segments to be ablated using insect pins, and superfine Vannas scissors (WPI Inc., Sarasota, FL, USA) were inserted approximately 1 mm into the body to damage the SRO or DNL.

Following recovery of spontaneous activity, between 6 and 40 h post-surgery, animals were tested for their performance in the following basic behaviours; postural maintenance, righting reflex (return to upright posture from side or back), horizontal crawling (upright), vertical crawling (up and down) and strike reflex (instigated by poking the prolegs). When necessary, crawling was evoked by anterograde dorsal stroking or gentle posterior squeezing. After behavioral evaluation, animals were anesthetized by chilling on ice, and SRO functionality was noted as described earlier (see Electrophysiology). In cases where ablation or the presence of full SRO function was unclear, the SRO morphology

was assessed by staining with 0.02% Janus Green in desheathing saline (Yack, 1993).

Based on the electrophysiological results, animals with non-functional SROs were considered to be a successful ablation, animals with correctly functional SROs were considered to be sham ablations and ambiguous cases were omitted from analysis. Animals were categorized according to their behavioral scores, and the difference between control and ablated animals in normal *versus* atypical behavior was tested using a Chi-Squared (χ^2) test.

Statistics

All statistical tests were carried out using Systat software (v. 10 or 11, SPSS, Chicago, IL, USA). In all cases except for SRO ablation, data were first tested for adherence to a normal distribution. Normally distributed data and data transformable to a normal distribution in accordance with Tukey's ladder (Tukey, 1977) were tested using parametric tests. Most tests involving tonic or phasic frequency used log-transformed frequency values. Log-transformed frequencies were normalized in tests of tonic activity *versus* displacement and phasic activity *versus* velocity. In the latter tests, velocities were also log-transformed. Tests of phasic activity *versus* start-position used normalized, but not log-transformed, phasic frequencies. Data that could not be transformed to a normal distribution were tested using non-parametric tests.

Correlation between endpoint of stretch and phasic activity was addressed differently. Because there were significant differences between the activity observed in different animals at given stretch velocities [Kruskal–Wallis test: by animal, $U_{0.05}(9,672)=508.386$, $P<0.0001$; by stretch velocity, $U_{0.05}(5,672)=521.538$, $P<0.0001$], we chose not to aggregate these data. Rather, we examined correlation between endpoint and phasic activity for each combination of animal and stretch velocity. Separate correlations between stretch endpoint and mean maximum phasic frequency were determined by animal and stretch velocity; these correlations were then averaged to observe the strength of correlation across multiple animals and stretch velocities.

RESULTS

Kinematics of typical behaviors

Because we were interested in the responses of the stretch receptor during behavior, we first observed animals to understand their normal range of motion (Fig. 3; Movies 1 and 2 in supplementary material) [also, for crawling (Belanger and Trimmer, 2000; Trimmer and Issberner, 2007); for striking (Walters et al., 2001)]. These motions were then classified according to amplitude and speed of stretch of the abdominal body wall, as determined from kinematic traces (Fig. 3Aiii,Biii).

The shortest range of motion was observed during the maintenance of posture; aside from making small pulsing movements, the animal essentially remained motionless. Net movements were close to zero and below levels observed during crawling. During crawling, the abdominal segments maintained a resting length (~5.0 mm) throughout stance phase but then shortened and re-lengthened during the swing phase (Fig. 3A). During the rapid strike reflex, animals that were squeezed gently on their terminal segment or on their anal claspers responded with a rapid strike to the area of stimulus with their head (Fig. 3B). Note that, in the case of both behaviors, kinematic results reveal periods of constant segment length and periods of rapid segment extension and contraction. Therefore, experiments involving stretching stimuli utilized sustained stretch stimuli, as well as stretch-and-hold stimuli, in order to cover the large range of activity observed during behavior.

Tonic and phasic response in *M. sexta*

To compare the *M. sexta* SRO with that of *A. pernyii*, we observed tonic output with the SRO stretched to different lengths (Fig. 4). Tonic activity increased as SRO length was increased (linear regression of log-transformed normalized frequencies to displacement; $t=23.8534$, $N=180$, $P<0.0001$). We also observed SRO output in response to stretch-and-hold stimuli (Fig. 5). We confirmed that the mean maximum phasic frequency increased with increasing stretch velocity (linear regression of log-transformed frequencies to log-transformed velocities; $t=14.942$, $N=38$, $P<0.0001$). We found that this log–log relationship was particularly linear at stretch velocities between 1 and 64 mm s^{-1}. As with *A. pernyii*, the phasic response was greater than what would be expected were the SRO to report displacement tonically. During stretches slower than 1 mm s^{-1}, phasic activity was almost indistinguishable from tonic responses expected at a similar length.

Wiener kernel characteristics

A traditional cross-correlation Wiener kernel analysis was used to quantitatively characterize the functional response of *Manduca* SRO (French and Marmarelis, 1999). To explore a full spectrum of behaviorally relevant stretch speeds, the stimulus f_c were varied and the responses to these stimuli were examined separately.

All of the afferents responded similarly to mechanical GWN stimuli. At f_c=12.5 Hz, all 12 afferents had similar biphasic first-order kernels (Fig. 6A). At higher f_c (25 Hz, 50 Hz), the SRO response was similar to the response at the lowest f_c (12.5 Hz), with the exception that the lag prior to the first positive peak was greater at higher frequencies. SRO second-order kernels were characterized by two peaks on the diagonal and by symmetrical off-diagonal valleys, similar to the 'four-eye' configuration described by Kondoh and colleagues (Kondoh et al., 1995) for velocity-sensitive afferents. As with the first-order kernels, the second-order kernels generated from all three f_c were similar, primarily differing in the degree of time lag prior to peaks and valleys (Fig. 6B).

Adaptation of tonic response

Past studies have measured tonic response at a fixed duration after changes in SRO length (Lowenstein and Finlayson, 1960; Weevers, 1965). Similarly, we report changes in tonic frequency observed at

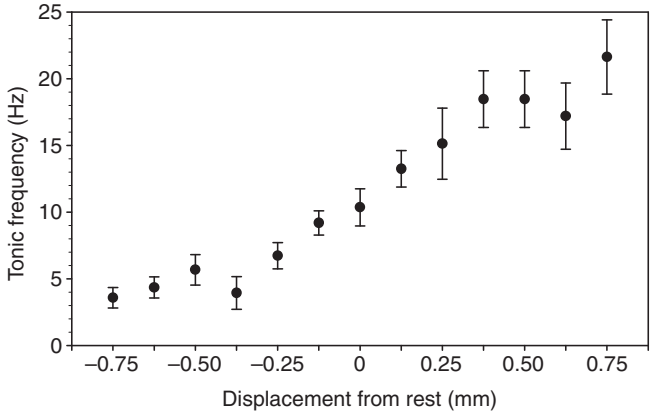

Fig. 4. Stretch receptor organ (SRO) tonic output frequency increased with displacement. *M. sexta* dorsal hemisegment was slowly stretched to randomly chosen lengths and held in that position for 20 s. Tonic frequency was averaged over an approximately 10 s period following termination of phasic activity. *N*=6 animals, 202 observations, error bars represent standard error.

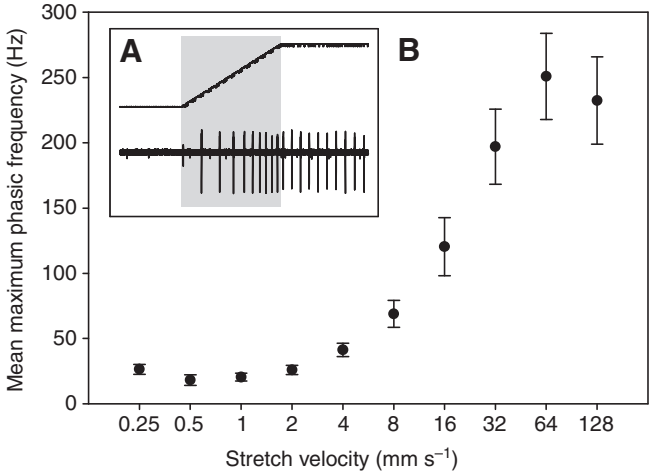

Fig. 5. Stretch receptor organ (SRO) phasic output increased with stretch velocity. (A) Recording of stretch-and-hold stimulus. *M. sexta* dorsal hemisegment was stretched 1 mm about the rest point at various velocities and then held briefly. The top trace is SRO length as measured by an ergometer. The bottom trace is SRO activity, as detected by an extracellular electrode. Maximum phasic frequency was calculated from the shaded area, beginning shortly before the start of a stretch and ending shortly after the end of that stretch. Representative sample. (B) Mean maximum phasic frequency at various stretch velocities. Mean maximum phasic frequency was determined from the mean of at least 10 consecutive stretches, where the maximum instantaneous frequency during stretch was determined for each separate stretch. *N*=5 animals, 48 observations, error bars represent standard error.

a fixed interval following changes in SRO length (Fig. 4). However, when the tissue was stretched and held at a fixed length, the output frequency decayed exponentially or rose exponentially following stretching or shortening, respectively (Fig. 7A).

In order to determine the factors influencing this tonic adaptation, we fitted each exponential decay to an exponential curve of the form $f(t)=A–B\times e^{-Ct}$, where $f(t)$ is the instantaneous tonic frequency over time (Fig. 7A). Quality of fit varied (Fig. 7B) but the median coefficient of determination (R^2) was 0.80, with 69% of fits having $R^2>0.50$. In real terms, the A parameter represented the steady-state level of tonic activity following the length change, the B parameter represented the degree of adaptation in tonic activity immediately following length change and the C parameter was the time constant indicating the duration of adaptation. Each (A,B,C) triplet was associated with a particular SRO length (Fig. 7C) and change in length (Fig. 7D).

We found a significant positive relationship between the tonic output level (A parameter) and segment length [linear regression of log(A) against length; N=58, t=2.717, P=0.0088] but not with a change in segment length [linear regression of log(A) against change in length; N=58, t=1.557, P=0.1252]. However, whereas there was no significant relationship between tonic adaptation and segment length [linear regression of log(B) against length; N=58, t=–1.199, P=0.2358], there was a significant negative relationship between tonic adaptation (B parameter) and change in segment length [linear regression of log(B) against change in length; N=58, t=–4.628, P<0.0001]. The time constant (C parameter) was not significantly affected by either segment length or change in length [linear regression of log(C) against length, N=58, t=–0.707, P=0.4827; change in length, N=58, t=–1.024, P=0.310].

Effects of displacement on phasic activity

Past studies have examined the phasic response to stretch velocity but not the effect of displacement on phasic response during stretch. We tested two ways by which displacement could be modified during stretch. First, we adjusted the start-point of the stretch, changing the span of the displacement but leaving the endpoint of the stretch fixed (Fig. 8). All results were normalized relative to the mean maximum phasic frequency observed in the case of a 1 mm span of stretch. Varying the span of the stretch between 25% and 150% of the control span (1 mm) did not have any effect on mean maximum phasic frequency [one-way analysis of variance (ANOVA); $F_{0.05}(5,28)$=0.3609, P=0.871].

Second, we adjusted the start- and endpoints of the stretch, leaving the span fixed (Fig. 9A). On a trial-by-trial basis, separated by animal and stretch velocity, we found a strong correlation between mean maximum phasic frequency and endpoint (mean of Pearson correlation coefficients, mean R^2=0.771). When these correlation coefficients were averaged across specimens stretched at a fixed velocity, the correlation between endpoint and phasic output was very strong at low velocities and decreased at higher velocities (mean of Pearson correlation coefficients; mean R^2 values: 2 mm s^{-1}, 0.934; 4 mm s^{-1}, 0.931; 8 mm s^{-1}, 0.895; 16 mm s^{-1}, 0.534; 32 mm s^{-1}, 0.601; 64 mm s^{-1}, 0.757). Thus, increasing the stretch endpoint position at lower stretch velocities resulted in an increased mean maximum phasic frequency; at higher stretch velocities, the endpoint position had a reduced effect on phasic output (Fig. 9B).

Behaviors following SRO ablation

To test whether the SRO is critical to the behavior of soft-bodied animals, we surgically ablated the SRO in the fourth abdominal segment in otherwise healthy animals. There was no significant difference in the observed behavior between unsuccessfully (sham) and successfully ablated animals in postural maintenance, righting reflex, upright crawling, vertical crawling and strike reflex (Table 1). We also observed that ablation of SROs in multiple, adjacent segments did not appear to have any effect on these behaviors.

DISCUSSION

In the present study, we examined the response of the lepidopteran SRO to mechanical stretching stimuli. We characterized the *Manduca* SRO as a tonic–phasic mechanosensor based on its response to functional tests (Figs 4 and 5) and these results were supported by GWN analysis (Fig. 6). In the following sections, we will discuss: (1) the implications of the change in tonic response over time and the change in phasic response over varying displacement, (2) the results of the Wiener kernel analysis and how the above results compare with the functional response of other proprioceptors and (3) propose functional roles for the longitudinal SRO in the context of specific animal behaviors.

Tonic adaptation in the time domain

As predicted by tests of raw displacement (Fig. 4), the steady-state tonic response of the SRO to slow stretch was directly related to segment length (Fig. 7C). However, tonic SRO activity adapts slowly to changes in segment length, taking over 45 s to reach 95% of total adaptation at the observed median time constant of 0.065. Based on our observation that SRO displacement, and not length, correlates significantly with the degree of adaptation (Fig. 7D), we conclude that SRO adaptation is largely a function of displacement, and not SRO length, for a period of approximately 45 s following length changes. Thus, body-segment length could be encoded by tonic activity in animals standing for long periods of time; however, during

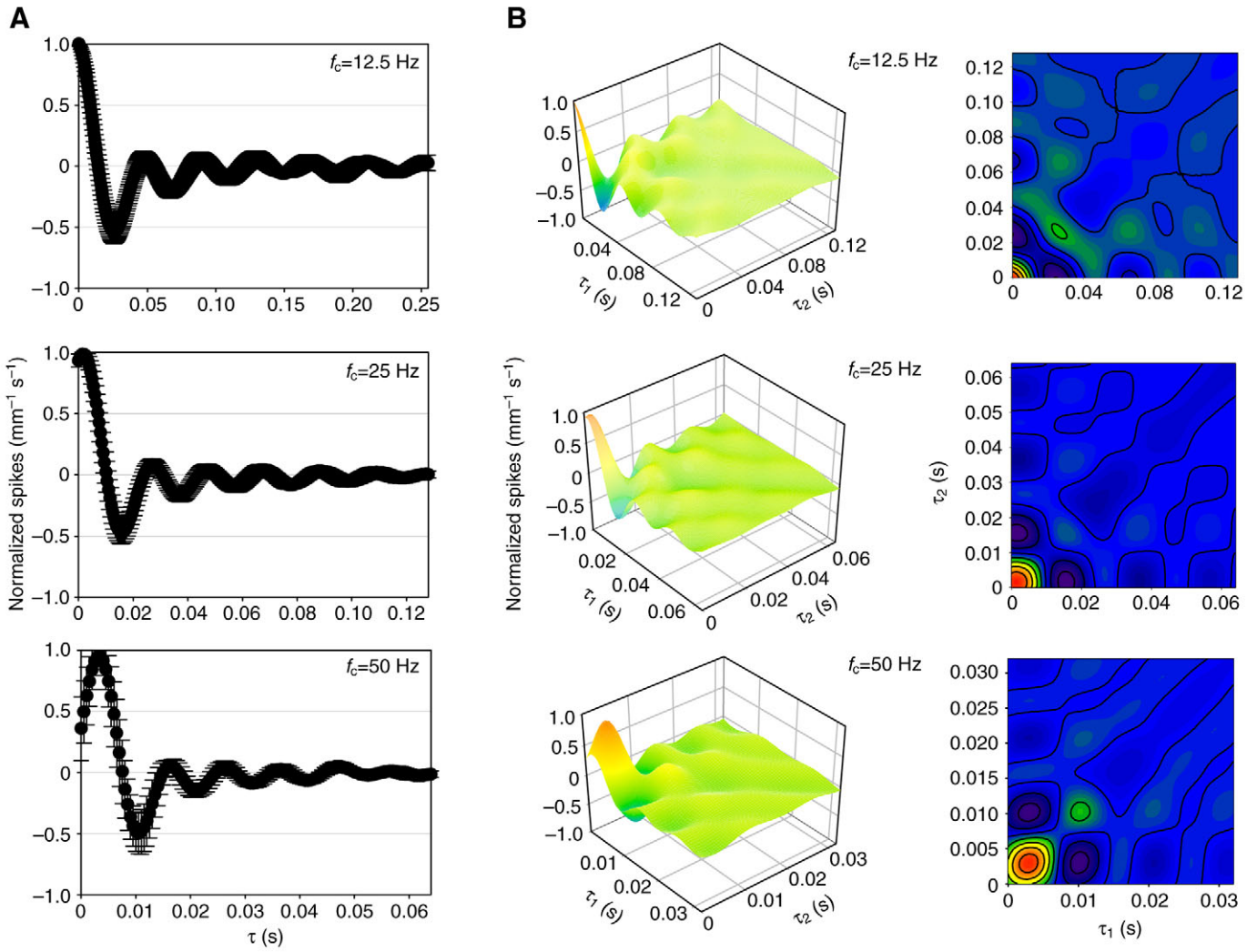

Fig. 6. Wiener kernels of stretch receptor organ (SRO) response to Gaussian white noise (GWN) are characteristic of a position–velocity sensor. Corresponding shapes of (A) first- and (B) second-order Wiener kernels from recordings of *M. sexta* SROs responding to GWN stimuli with cutoff frequency (f_c)=12.5, 25 and 50 Hz. Amplitude represents normalized spikes mm^{-1} s^{-1} of lag. *N*=12 animals.

any movement, patterned or otherwise, it seems unlikely that the stretch receptor can accurately signal body segment length in the short term.

Although neither SRO length nor change in length explain the time constant of adaptation (Fig. 7C,D), we observe that SRO adaptation is similar to the adaptation of passive *Manduca* muscle to mechanical stimuli (Woods et al., 2008). It is possible that SRO adaptation arises from the internal mechanical properties of the stretch receptor muscle fiber. However, we have not ruled out other explanations such as neurochemical modulation as observed in acoustic sensory systems (Herz et al., 2005). Such a mechanism would permit the rate of adaptation to be modulated by factors independent of movement such as by the stretch receptor motoneuron (Weevers, 1966b).

Phasic response in displacement domain

We showed that the phasic response depends on the endpoint of the stretch (Fig. 9) but it is not affected by the start-point of the stretch (Fig. 8). These results suggest that as an abdominal segment stretches rapidly, SRO activity will immediately increase with position, even at constant velocity. Past tests of the response by the SRO to stretch velocity typically involved stretching the SRO fixed distances between two points at varying velocities. Finlayson and Lowenstein measured activity resulting from sinusoidal stimulation (Lowenstein and Finlayson, 1960); our present study (in Fig. 5) and the study by Weevers, measured activity resulting from fixed-velocity stretch-and-hold patterns (Weevers, 1965). However, previous stretch-and-hold experiments did not test the effect of changes in the start- and endpoints of the stretch. Within the range of stretches used in the present study, we find the unexpected result that span does not affect phasic output.

First- and second-order Wiener kernels

The first-order kernel of an SRO afferent represents its response to an impulse change in length of the SRO-bearing segment. We observed a consistently biphasic first-order kernel (Fig. 6A). The initial positive peak represents the increase in activity in response to SRO stretch (length increase), indicating that the SRO responds positively to stretch and not to contraction or relaxation. The first-order kernel can also be interpreted as the mean stimulus seen

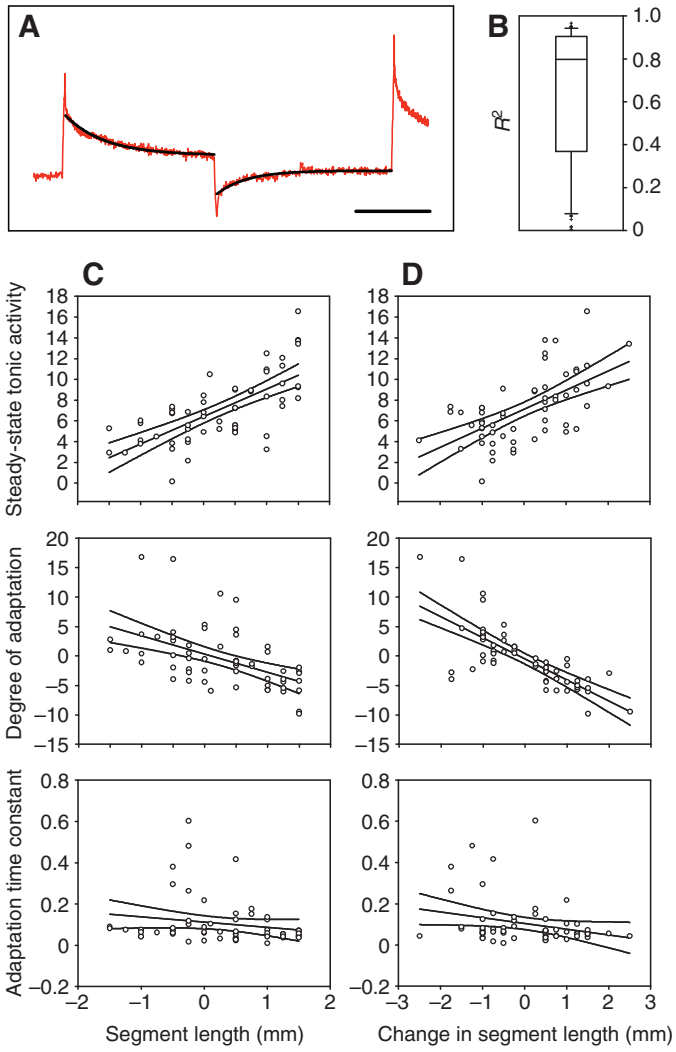

Fig. 7. Tonic adaptation correlated more strongly with a change in stretch receptor organ (SRO) length rather than length itself. (A) Example of tonic adaptation. Following a slow (non-phasic activity-inducing) change in SRO length, tonic activity initially changed to reflect the new SRO length and then adapted in the opposite direction of the initial change. The black line overlying the red trace shows fit to adaptation. Scale bar=30 s. (B) Quality of fit as characterized by R^2 values. Median R^2 was 0.8. (C) The length of SRO had a significant effect on the level of tonic activity but not on the degree of adaptation. (D) A change in the length of SRO had a significant effect on tonic adaptation but not on the level of tonic activity. Neither length nor change in length had a significant effect on the decay time constant.

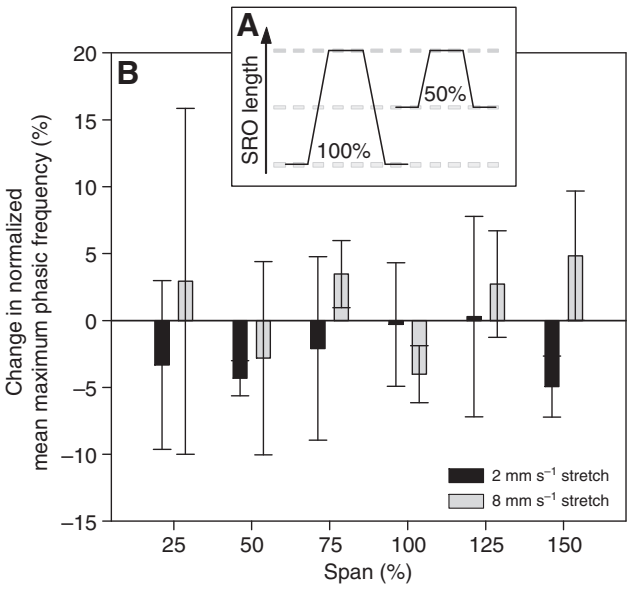

Fig. 8. Span of stretch did not affect phasic output. (A) The endpoint of a stretch was held constant and the start-point was varied in order to see if the span of a stretch affected the phasic output. (B) The data represent the stretch receptor organ (SRO) mean maximum phasic frequency following stretch of the fourth abdominal hemisegment in fifth-instar second day *M. sexta*. In all cases, endpoint of stretch was held at 0.5 mm over the rest point, with the total span varied between 25% and 150% of the control span (1 mm). In all other respects, this method was identical to previous phasic stretch-and-hold experiments. *N*=3 animals, 40 observations, error bars represent standard error.

immediately before a spike (Marmarelis, 1978). In that way, we note that the negative peak seen after the initial positive peak indicates that the receptor also responds to changes (negative-to-positive) in stretch stimulus, i.e. it responds to stretch velocity. This positive-led biphasic response matched the characteristic curve of other position–velocity mechanosensors (Gamble and DiCaprio, 2003; Kondoh et al., 1995).

Second-order kernels represent the non-linear interactions between the current response and two time points in the stimulus history, τ_1 and τ_2. SRO second-order kernels were uniformally characterized by two peaks on the diagonal $\tau_1=\tau_2$ and symmetrical off-diagonal troughs (Fig. 6B). The on-diagonal peaks and troughs represent amplitude-dependent non-linearities, which can be compared directly with the linear system response of the first-order kernel (Marmarelis, 1978). For example, in the case of f_c=12.5 Hz, the on-diagonal peak observed at $\tau_1=\tau_2$=25 ms in the second-order kernel corresponds to a trough in the first-order kernel at the same time lag, indicating a rectifying non-linearity. Off-diagonal peaks and troughs represent interactions between historical stimuli and the current response. For example, whereas a high amplitude stimulus immediately promotes a response spike according to high amplitude in the first-order kernel at τ=0 s, the interaction of the input at lag τ_1=0 s with the input at lag τ_2=25 ms results in a negative value, reducing the likelihood of a spike; i.e. a high amplitude stimulus occurring 25 ms in the past reduces the likelihood of a spike due to an immediate high amplitude stimulus. The substantially reduced likelihood of a spike moments after a high amplitude signal may be indicative of the refractory period seen after spiking events.

Comparison with other proprioceptors

The *Manduca* SRO functions similarly to proprioceptors described in other invertebrates. The most straightforward comparison is with the *Antherea* SRO, which is similar anatomically to that of *Manduca* (Lowenstein and Finlayson, 1960; Weevers, 1966a). *Antherea pernyii* SROs produced tonic and phasic outputs very similar to that of *Manduca*, although Weevers (Weevers, 1965) also described a phasic component due to stretch acceleration in the *Antherea* SRO that we did not observe in *Manduca* SRO. In other animals, similarities are seen in output but not structure. In crustaceans, for example, the MRO response is tonic–phasic, like that of the *Manduca* SRO; however, unlike in *Manduca*, the crustacean tonic

Table 1. Comparing the behavior of animals with ablated stretch receptor organs (SROs) with the behavior of animals with sham ablations

Behavior	*P*-value
Postural maintenance	0.372
Righting reflex	0.301
Horizontal crawling (upright)	0.648
Vertical crawling (up and down)	*
Strike reflex	0.377

A Chi-squared test was used to compare prevalence of atypical behaviors in successful *versus* sham ablations. Six to 40 h following an attempted SRO ablation, animals were tested on the above behaviors. Any deviations from typical behavior were noted. Animals were then killed and tested for SRO function. Animals with non-functional or clearly malfunctioning SROs were marked as successful ablations, animals with functional SROs were marked as sham ablations and unclear cases were omitted. *=No abnormalities in vertical crawling were observed in any of the animals. *N*=8 successful ablations, *N*=17 sham ablations.

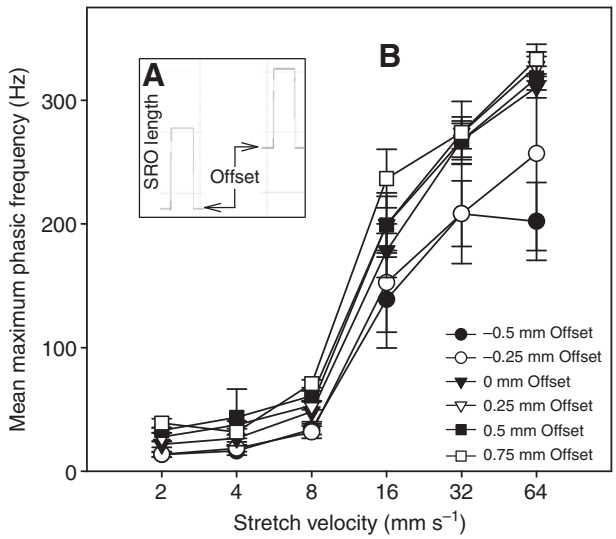

Fig. 9. Stretch receptor organ (SRO) phasic output decreased with decreased endpoint length. (A) In this series of experiments, the span of stretch was held constant and the start- and endpoints of stretch were varied about the rest length of the SRO. (B) For a given endpoint level, the mean, maximum phasic frequency was determined from at least 10 stretches at a particular start-point/endpoint combination. This was tested with six stretch velocities: 2, 4, 8, 16, 32 and 64 mm s^{-1}. *N*=5 animals, 672 observations, error bars represent standard error.

and phasic responces are divided between two wholly separate fibers, the slow- and fast-adapting muscle fibers (Eyzaguirre and Kuffler, 1955). Among the insects, a particularly interesting and well-reported case comes in the form of the locust CTMRO, which reports tonically proportional to angle but dynamically alters its response to nearby non-muscle-associated proprioceptors (Braunig and Hustert, 1985). Although there are no nearby chordotonal or strand receptors in the case of *Manduca*, it is an interesting and yet unexplored question as to whether *Manduca* SROs directly influence each others' afferent responses.

As described previously, GWN analysis has been used extensively for characterizing mechanosensors. Our results describe a rectifying position- and velocity-sensitive afferent; a characterization that agrees with our own electrophysiology results as well as previous studies characterizing lepidopteran stretch receptors (Lowenstein and Finlayson, 1960; Weevers, 1966a). Furthermore, our results are very similar to those of two non-muscle-associated sensors, the crab CB-chordotonal spiking neurons (Gamble and DiCaprio, 2003) and position-velocity sensing locust femoral chordotonal organs (Kondoh et al., 1995).

Additionally, our findings on adaptation have precedent. In locust, both the muscle-associated MROs and non-muscle-associated strand receptors adapt to constant stimuli (Braunig and Hustert, 1985). As already noted, crustacean MROs are functionally segregated as either slow- or fast-adapting fibers (Cattaert and Le Ray, 2001). However, unlike the fast-adapting fiber of crustacean MROs (Eyzaguirre and Kuffler, 1955), the *Manduca* SRO did not have a threshold for phasic spiking (Fig. 8).

SRO function in the context of postural maintenance

We have defined 'postural maintenance' as the behavior of the animal during a stance position even when faced with external forces. When a single abdominal body segment stops moving longitudinally its constituent SROs should cease to produce phasic activity (Fig. 5). Following tonic adaptation (Fig. 7), the tonic activity generated by these SROs could provide stable information about the length of the body segment (Fig. 4). By comparing spike rates from adjacent segments and across the longitudinal body axis, a somatotopic map of relative body position could be formed in the CNS, similar to that of the sensory hairs on *M. sexta* prolegs (Levine et al., 1985; Peterson and Weeks, 1988) and on the abdominal body surface (Levine et al., 1985).

One mechanism for postural maintenance could be through sensing strains induced by adjacent segments. If a segment is not held in sufficient tension by its intersegmental muscles, it will begin to lengthen under the force exerted by adjacent segments. This local increase in stretch would cause an increase in SRO tonic activity and could be used to restore segment length through a stretch reflex (Tamarkin and Levine, 1996). In this way, the SRO is a strain sensor that indirectly measures tension on the body overall. If strain is related to overall body tension, this could also provide a mechanism to regulate turgor.

SRO function in the context of strike response

Our findings suggest a specific role for the SRO in controlling striking behavior. Strikes to stimuli at the posterior segments are rapid and precise, targeting the stimulus at specific points on the body (Walters et al., 2001). During the strike response, the sides of the abdominal segments stretch rapidly, shortening at rates around 20 mm s^{-1} and lengthening at rates double this (Fig. 3B). By contrast, noxious stimuli applied to the thoracic and anterior abdominal segments elicit a slower movement of the body away from the source of the stimulus (Walters et al., 2001).

In the range of stretch velocities observed during strikes (between 5 and 50 mm s^{-1}), phasic activity increases very rapidly with velocity (Fig. 5) and somewhat less rapidly with increases in SRO length (Fig. 9). Our results predict that the combination of these two factors will cause a high frequency phasic response as the SRO is stretched to the end of its dynamic range. This would provide a powerful signal indicating the maximum strain of the body segment. Furthermore, this signal would strongly excite ipsilateral intersegmental muscles through the stretch reflex, bilaterally slowing the rate of stretch on the segment (Tamarkin and Levine, 1996) and generating negative feedback control during this rapid behavior.

SRO function in the context of crawling

One question in this study was whether or not the SRO plays a proprioceptive role during crawling. Sensory feedback can be used to alter locomotion in crawling animals (Weevers, 1965) and can coordinate condition-dependent reflexes during crawling (Belanger et al., 2000). However, because tonic activity is a poor indicator of body segment length for nearly 45 s following a change in segment length, the SRO cannot provide an accurate measure of body length during crawling. Phasic activity may influence crawling by reporting the rapidity of stretch during a crawl cycle; however, we have shown that the phasic response is positively influenced by length, an effect that will skew the inferred rate of stretch. Furthermore, we found that ablation of abdominal SROs does not have a significant observable effect on crawling or any of the other major activities we tested in *Manduca* (Table 1). Therefore, despite the position and size of the SRO, which are suggestive of a role in crawling, our results do not support the hypothesis that the SRO plays a critical role in the coordination of crawling.

Alternative roles of SROs in soft-bodied animals

It is possible that the SRO contributes to elements of behavior that are not directly visible. For example, cat deafferentation results in changes that can be detected by electromyography but not by the kinematics of undisturbed and supported walking on a treadmill (Hiebert and Pearson, 1999). Fields, observing similar temporal lag in response to position in the crustacean MRO, proposed that the stretch receptor acts as an error detector rather than a length-measuring sensor during certain animal behaviours (Fields, 1966). However, the lack of any behavioral deficit in SRO-ablated *Manduca* shows that a complete complement of SROs is not essential for most tasks; if information from the SRO is used for motion control at all, it must be highly redundant or easily compensated by other sensory systems.

Although not the focus of the present study, it is possible that a developmental role is played by the longitudinal SROs in *Manduca sexta*. Body size is a factor in gating final-instar molting in *M. sexta* (Nijhout, 2003), and abdominal stretch receptors are used for clearing size-regulated checkpoints in *Rhodnius prolixus* (Wigglesworth, 1934) and *Oncopeltus fasciatus* (Nijhout, 1979). However, unlike in *O. fasciatus,* molting in *Manduca* cannot be induced prematurely by abdominal inflation (Nijhout, 1981), so size monitoring by SROs in *Manduca* has yet to be demonstrated.

One possible behavioral role for SROs during crawling is that tonic and phasic output are synthesized into a form of feature detection useful for signaling the status of a crawl cycle. Such feature detection mechanisms have been described in a variety of organisms, including crickets (Marsat and Pollack, 2006), electric eels (Oswald et al., 2004) and humans (Lesica and Stanley, 2004). Although we do not know if SROs play this role in *Manduca*, SRO responses to repetitive and complex stretch cycles (derived from the kinematics of crawling caterpillars) reveal consistent patterns of activity (e.g. Fig. 1C). These patterns might convey features that are not essential for immediate motor activity (and therefore cannot be resolved by SRO ablation) but are nonetheless useful for adapting to environmental changes. This possibility is the subject of an ongoing study.

LIST OF ABBREVIATIONS

CTMRO	coxo-trochantal muscle receptor organ (locust)
DNL	dorsal lateral nerve
GWN	Gaussian white noise
MRO	muscle receptor organ (crustacean)
SRO	stretch receptor organ (lepidopteran)
SRSN	stretch receptor sensory neuron

This research was supported by National Science Foundation grants IBN-0117135 and IOS-0718537 to B.A.T., and by a W. M. Keck Foundation Science and Engineering Program grant *Biomimetic Technologies for Soft-bodied robots* to B.A.T. Thanks to the Tufts Biology Writing Club for feedback during preparation of this manuscript. Many thanks, also, to the University of Southern California's Biomedical Simulations Resource (BMSR) center for providing their LYSIS 7.1 software free of charge and on the Internet (http://bmsrs.usc.edu/). The development of LYSIS is funded by Grant RRO1861 from the National Center for Research Resources of the National Institutes of Health. The BMSR holds the copyright of LYSIS.

REFERENCES

Alexandrowicz, J. S. (1967). Receptor organs in thoracic and abdominal muscles of crustacea. *Biol. Rev. Camb. Philos. Soc.* **42**, 288-326.
Anwyl, R. (1972). Structure and properties of an abdominal stretch receptor in *Rhodnius-prolixus*. *J. Insect Physiol.* **18**, 2143-2154.
Beckel, W. E. (1958). The morphology, histology and physiology of the spiracular regulatory apparatus of *Hyalophora cecropia*. *Proc. 10th Int. Congr. Entomol.* **2**, 87-115.
Belanger, J. H. and Trimmer, B. A. (2000). Combined kinematic and electromyographic analyses of proleg function during crawling by the caterpillar *Manduca sexta*. *J. Comp. Physiol. A* **186**, 1031.
Belanger, J. H., Bender, K. J. and Trimmer, B. A. (2000). Context dependency of a limb withdrawal reflex in the caterpillar *Manduca sexta*. *J. Comp. Physiol. A* **186**, 1041-1048.
Bell, R. A. and Joachim, F. G. (1976). Techniques for rearing laboratory colonies of tobacco hornworms and pink bollworms Lepidoptera-sphingidae-gelechiidae. *Ann. Entomol. Soc. Am.* **69**, 365-373.
Bouverot, P. (1978). Control of breathing in birds compared with mammals. *Physiol. Rev.* **58**, 604-655.
Braunig, P. and Hustert, R. (1983). Proprioceptive control of a muscle receptor organ in the locust leg. *Brain Res.* **274**, 341-343.
Braunig, P. and Hustert, R. (1985). Actions and Interactions of proprioceptors of the locust hind leg Coxo-trochanteral joint.1. Afferent responses in relation to joint position and movement. *J. Comp. Physiol. A* **157**, 73-82.
Cattaert, D. and Le Ray, D. (2001). Adaptive motor control in crayfish. *Prog. Neurobiol.* **63**, 199-240.
DiCaprio, R. A. (2003). Nonspiking and spiking proprioceptors in the crab: nonlinear analysis of nonspiking TCMRO afferents. *J. Neurophysiol.* **89**, 1826-1836.
Dietz, V., Muller, R. and Colombo, G. (2002). Locomotor activity in spinal man: significance of afferent input from joint and load receptors. *Brain* **125**, 2626-2634.
Eyzaguirre, C. and Kuffler, S. W. (1955). Processes of excitation in the dendrites and in the soma of single isolated sensory nerve cells of the lobster and crayfish. *J. Gen. Physiol.* **39**, 87-119.
Fields, H. L. (1966). Proprioceptive control of posture in the crayfish abdomen. *J. Exp. Biol.* **44**, 455-468.
Fields, H. L. and Kennedy, D. (1965). Functional role of muscle receptor organs in crayfish. *Nature* **206**, 1235-1237.
French, A. S. (1980). Sensory transduction in an insect mechanoreceptor-linear and non-linear properties. *Biol. Cybern.* **38**, 115-123.
French, A. S. and Marmarelis, V. Z. (1999). Nonlinear analysis of neuronal systems. In *Modern Techniques in Neuroscience Research* (ed. U. Windhorst and H. Johnannson), pp. 627-640. Heidelberg: Springer-Verlag.
French, A. S. and Wong, R. K. S. (1977). Nonlinear analysis of sensory transduction in an insect mechanoreceptor. *Biol. Cybern.* **26**, 231-240.
Gamble, E. R. and DiCaprio, R. A. (2003). Nonspiking and spiking proprioceptors in the crab: white noise analysis of spiking CB-chordotonal organ afferents. *J. Neurophysiol.* **89**, 1815-1825.
Gwadz, R. W. (1969). Regulation of blood meal size in mosquito. *J. Insect Physiol.* **15**, 2039-2044.
Herz, A. V. M., Benda, J., Gollisch, T., Machens, C. K., Schaette, R., Schütze, H. and Stemmler, M. B. (2005). Auditory processing of acoustic communication signals. In *Methods in Insect Sensory Neuroscience* (ed. T. A. Christensen), pp. 129-156. Boca Raton, FL: CRC Press.
Hiebert, G. W. and Pearson, K. G. (1999). Contribution of sensory feedback to the generation of extensor activity during walking in the decerebrate cat. *J. Neurophysiol.* **81**, 758-770.
Kondoh, Y., Okuma, J. and Newland, P. L. (1995). Dynamics of neurons controlling movements of a locust hind leg: Wiener Kernel analysis of the responses of proprioceptive afferents. *J. Neurophysiol.* **73**, 1829-1842.
Kroller, J. (1993). Reverse correlation-analysis of the stretch response of primary muscle-spindle afferent-fibers. *Biol. Cybern.* **69**, 447-456.
Kuffler, S. W. (1954). Mechanisms of activation and motor control of stretch receptors in lobster and crayfish. *J. Neurophysiol.* **17**, 558-574.
Lesica, N. A. and Stanley, G. B. (2004). Encoding of natural scene movies by tonic and burst spikes in the lateral geniculate nucleus. *J. Neurosci.* **24**, 10731-10740.
Levine, R. B., Pak, C. and Linn, D. (1985). The structure, function and metameric reorganization of somatotopically projecting sensory neurons in *Manduca sexta* larvae. *J. Comp. Physiol. A* **157**, 1-13.
Libby, J. (1961). The nervous system of certain abdominal segments and the innervation of the male reproductive system and genitalia of *Hyalophora cecropi*. *Ann. Entomol. Soc. Am.* **54**, 887-896.
Lowenstein, O. and Finlayson, L. H. (1960). The response of the abdominal stretch receptor of an insect to phasic stimulation. *Comp. Biochem. Physiol.* **1**, 56-61.

Marmarelis, V. Z. (1978). *Analysis of Physiological Systems: The White-Noise Approach*. New York, NY: Plenum Press.
Marmarelis, V. Z. and Mccann, G. D. (1973). Development and application of white-noise modeling techniques for studies of insect visual nervous-system. *Kybernetik* **12**, 74-89.
Marsat, G. and Pollack, G. S. (2006). A behavioral role for feature detection by sensory bursts. *J. Neurosci.* **26**, 10542-10547.
Nijhout, H. F. (1979). Stretch-induced molting in Oncopeltus-fasciatus. *J. Insect Physiol.* **25**, 277-281.
Nijhout, H. F. (1981). Physiological control of molting in insects. *Am. Zool.* **21**, 631-640.
Nijhout, H. F. (2003). The control of body size in insects. *Dev. Biol.* **261**, 1-9.
O'Hagan, R., Chalfie, M. and Eric, A. (2005). Mechanosensation in *Caenorhabditis elegans*. In *International Review of Neurobiology*, vol. 69, pp. 169-203. San Diego, CA: Academic Press.
Osborne, M. P. and Finlayson, L. H. (1965). An electron microscope study of the stretch receptor of *Antheraea pernyi* (Lepidoptera, saturniidae). *J. Insect Physiol.* **11**, 703-710.
Oswald, A. M. M., Chacron, M. J., Doiron, B., Bastian, J. and Maler, L. (2004). Parallel processing of sensory input by bursts and isolated spikes. *J. Neurosci.* **24**, 4351-4362.
Paintal, A. S. (1973). Vagal sensory receptors and their reflex effects. *Physiol. Rev.* **53**, 159-227.
Peterson, B. A. and Weeks, J. C. (1988). Somatotopic mapping of sensory neurons innervating mechanosensory hairs on the larval prolegs of *Manduca sexta*. *J. Comp. Neurol.* **275**, 128-144.
Recio-Spinoso, A., Temchin, A. N., van Dijk, P., Fan, Y. H. and Ruggero, M. A. (2005). Wiener-kernel analysis of responses to noise of chinchilla auditory-nerve fibers. *J. Neurophysiol.* **93**, 3615-3634.
Snodgrass, R. E. (1935). *Principles of Insect Morphology*. New York, NY: McGraw-Hill.
Stein, R. B., Misiaszek, J. E. and Pearson, K. G. (2000). Functional role of muscle reflexes for force generation in the decerebrate walking cat. *J. Physiol.* **525**, 781-791.
Sumbre, G., Fiorito, G., Flash, T. and Hochner, B. (2005). Motor control of flexible octopus arms. *Nature* **433**, 595-596.
Syntichaki, P. and Tavernarakis, N. (2004). Genetic models of mechanotransduction: the nematode *Caenorhabditis elegans*. *Physiol. Rev.* **84**, 1097-1153.
Tamarkin, D. A. and Levine, R. B. (1996). Synaptic interactions between a muscle-associated proprioceptor and body wall muscle motor neurons in larval and adult *Manduca sexta*. *J. Neurophysiol.* **76**, 1597-1610.
Trimmer, B. and Issberner, J. (2007). Kinematics of soft-bodied, legged locomotion in *Manduca sexta* larvae. *Biol. Bull.* **212**, 130-142.
Trimmer, B. A. and Weeks, J. C. (1991). Activity-dependent induction of facilitation, depression, and post-tetanic potentiation at an insect central synapse. *J. Comp. Physiol. A* **168**, 27-43.
Tukey, J. W. (1977). *Exploratory Data Analysis*. Reading, MA: Addison-Wesley.
Tytell, E. D. and Cohen, A. H. (2008). Rostral *versus* caudal differences in mechanical entrainment of the lamprey central pattern generator for locomotion. *J. Neurophysiol.* **99**, 2408-2419.
Walters, E. T., Illich, P. A., Weeks, J. C. and Lewin, M. R. (2001). Defensive responses of larval *Manduca sexta* and their sensitization by noxious stimuli in the laboratory and field. *J. Exp. Biol.* **204**, 457-469.
Weevers, R. d. G. (1965). Proprioceptive reflexes and coordination of locomotion in the caterpillar of *Antheraea pernyi* (Lepidoptera). In *The Physiology of The Insect Central Nervous System* (ed. J. E. Treherne and J. W. L. Beament), pp. 113-124. New York: Academic Press.
Weevers, R. D. (1966a). The physiology of a lepidopteran muscle receptor. I. The sensory response to stretching. *J. Exp. Biol.* **44**, 177-194.
Weevers, R. D. (1966b). The physiology of a lepidopteran muscle receptor. II. The function of the receptor muscle. *J. Exp. Biol.* **44**, 195-208.
Weevers, R. D. (1966c). The physiology of a lepidopteran muscle receptor. III. The stretch reflex. *J. Exp. Biol.* **45**, 229-249.
Wigglesworth, V. B. (1934). The physiology of ecdysis in *Rhodnius prolixus* (Hemiptera). II. Factors controlling moulting and 'metamorphosis'. *Q. J. Microsc. Sci.* **77**, 191-222.
Woods, W. A., Fusillo, S. J. and Trimmer, B. A. (2008). Dynamic properties of a locomotory muscle of the tobacco hornworm *Manduca sexta* during strain cycling and simulated natural crawling. *J. Exp. Biol.* **211**, 873-882.
Yack, J. E. (1993). Janus Green B as a rapid, vital stain for peripheral nerves and chordotonal organs in insects. *J. Neurosci. Methods* **49**, 17-22.